J Mater Sci (2008) 43:5998–6004
DOI 10.1007/s10853-008-2660-8

Atomic force microscopy tip torsion contribution to the measurement of nanomechanical properties

C. M. Almeida · R. Prioli

Received: 13 December 2007 / Accepted: 15 April 2008 / Published online: 13 August 2008
© Springer Science+Business Media, LLC 2008

Abstract The nanomechanical properties of polymethyl methacrylate and indium phosphide were measured with an atomic force microscope and a nanoindentation system. The elastic moduli measured with the atomic force microscope are in good agreement with the values obtained with the nanoindentation system. The hardness is shown to be affected by the tip radius used in our experiments. The cantilever vertical and lateral movements were independently analyzed during nanoindentation, and the tip torsion can be attributed to a change from elastic to plastic deformation regimes of materials during force microscopy nanoindentation. An analysis of the lateral movement of the laser beam associated with the cantilever torsion was used to determine the material yield stress.

Introduction

The understanding of deformation mechanisms of materials under pressure is essential to the development of new devices. Since the size of the devices has reached the nanometer level, a proper characterization technique has to be developed so that the materials mechanical characterization can be fully performed in such a small scale. Nanoindenters have been developed and used with great success on the characterization of materials using forces ranging from a few μN to several mN. Within this force range, a lot of information on the deformation mechanisms of materials under load can be obtained. To be able to understand the initial steps of the deformation processes, smaller forces are needed. The capability to measure forces in the nN range makes the atomic force microscope (AFM) an interesting tool to measure mechanical properties of materials.

The measurement of nanomechanical properties of materials with AFM has become possible due to the precise control of the microscope tip position and forces applied between the tip and the studied surface, as shown by Bhushan and Koinkar [1]. AFM operational modes have been developed in the last few years giving new information regarding the materials properties. The phase image in tapping mode gives information about the materials elasticity and adhesion [2], the force modulation technique allows the subsurface defects visualization and the mapping of the materials elasticity in a surface [3, 4]. The nanoindentation of the AFM tip on a surface allows the determination of the materials hardness and elasticity [5]. The tapping mode phase image and the force modulation technique are very sensitive to the stiffness and resonance frequency of the microscope cantilever and a quantitative determination of the materials elastic modulus is hardly obtained. On the other hand, nanoindentations with AFM are sensitive to the cantilever's stiffness and to the normal bending and lateral torsion of the microscope cantilever. If a proper analysis of the microscope cantilever movement is performed, the quantitative determination of the materials hardness and elastic modulus can be obtained.

In this work, the mechanical properties of polymethyl methacrylate (PMMA) and indium phosphide (InP) were measured with atomic force microscopy nanoindentation. A careful analysis of the AFM cantilever movement during the nanoindentation was performed. The cantilever vertical and lateral movements were independently acquired and analyzed. The quantitative determination of the materials

C. M. Almeida · R. Prioli (✉)
Departamento de Física, Pontifícia Universidade Católica do Rio de Janeiro, Marques de São Vicente 225, Rio de Janeiro 22453-900, Rio de Janeiro, Brazil
e-mail: prioli@vdg.fis.puc-rio.br

hardness and elastic modulus were obtained by the analysis of the vertical movement of the cantilever. The analysis of the AFM cantilever lateral torsion allowed the quantitative determination of the materials yield stress. It is shown in this work that a careful analysis of the AFM cantilever movement gives information about the initial steps of plastic deformation of materials under load.

Experimental procedures

The nanomechanical characterization of PMMA and InP was done using an atomic force microscope. Force curve measurements were performed with an AFM (MultiMode, Veeco, Santa Barbara, CA) controlled with a Nanoscope IIIa electronics operated in air. The sample located on top of the microscope piezoelectric ceramic was pushed towards the AFM tip while the cantilever vertical deflection was recorded. The AFM software plots the vertical piezo (sample) displacement (Δz) versus the cantilever vertical deflection response (ΔV) in volts. To convert the cantilever vertical deflection response given in volts into cantilever displacement in nm (Δs), the cantilever sensitivity was used. It was measured in a sapphire sample that was used as an 'infinitely' hard material. The force applied by the cantilever was calculated by multiplying the cantilever vertical displacement by the cantilever normal bending constant. The deformation of the surface under load (Δh) was obtained by $\Delta h = \Delta z - \Delta s$ [6]. Thus, nanoindentation curves were achieved. The unload part of the nanoindentation curve was fitted using the Oliver & Pharr model so that the materials elastic modulus and hardness were determined [7].

To record simultaneously the vertical and lateral movement of the cantilever during the nanoindentation process a LabView routine was used. The vertical and lateral signals were accessed through a signal access module (Veeco).

The cantilever's choice was based on the sensitivity measurement in force curves obtained at different materials. The measurement of materials mechanical properties depends on how the cantilever bends due to the contact with the surface. The sensitivity is the ratio between the cantilever vertical deflection and the piezo displacement. A contact mode Si_3N_4, a Si, and a stainless steel cantilever equipped with a diamond tip were tested. The cantilever's sensitivity measurements at several materials are shown in Fig. 1. The stainless steel cantilever presents the largest sensitivity variation in the range of the elastic modulus studied. Therefore, the stainless steel cantilever was chosen to test the materials mechanical properties. The stainless steel cantilever was then carefully calibrated so that quantitative elasticity and hardness data could be obtained.

To calibrate the cantilever, the cantilever dimensions and resonance frequency were measured. The cantilever length and width were measured with an AxioPlan 2ie optical microscope (Carl Zeiss Inc., Thornwood, NY), and the resonance frequency was obtained with the force microscope software. A normal bending constant of 313 N/m was measured for a cantilever resonance frequency of 60 KHz. To estimate the tip area function, the diamond tip radius was measured. A CrN tip tester [8] was imaged by AFM operated in tapping mode and a blind reconstruction method was used [9]. A tip radius of 80 nm was obtained.

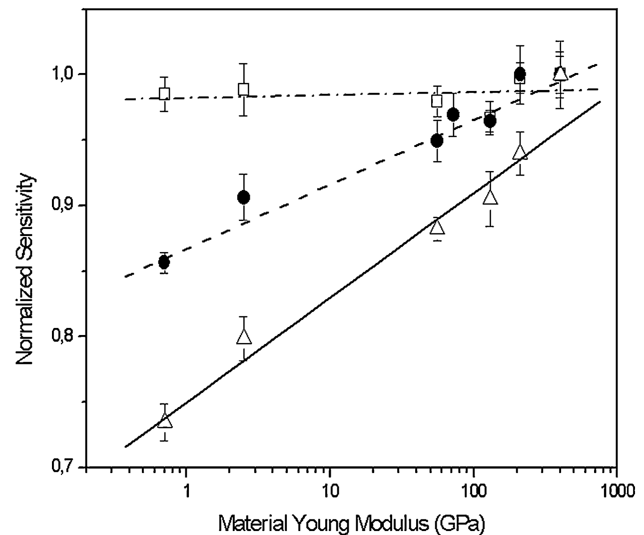

Fig. 1 Normalized cantilever sensitivity versus elastic modulus for different cantilevers ((□) a contact mode Si_3N_4 cantilever, (●) a tapping mode Si cantilever, and (△) a stainless steel cantilever)

Nanoindentation experiments using a Triboscope Nanomechanical Testing System (Hysitron Inc, Minneapolis, MN) were performed to compare the results with the ones obtained by AFM nanoindentation. A conospherical diamond probe tip with a curvature radius of 260 nm was used in all measurements. A nanoindentation load function with three segments was used. The load was linearly increased from zero to the maximum force in an interval of 5 s, the maximum force was then applied for 2 s (hold time), and finally the load was linearly decreased until zero in 5 s.

A viscoelastic PMMA sample supplied with our Triboscope was used without any further sample preparation step. A semi-insulating epi-ready InP (100) wafer (InPACT Inc., Fremont, CA) was heated at 630 °C in a metal organic vapor phase epitaxy AIX200 reactor and a 500 nm InP buffer layer was grown to minimize surface defects on InP. The InP samples were then directly placed on the equipments for the nanoindentation study.

Results

Nanoindentation curves of PMMA and InP performed with the Triboscope nanoindenter are shown in Fig. 2. A

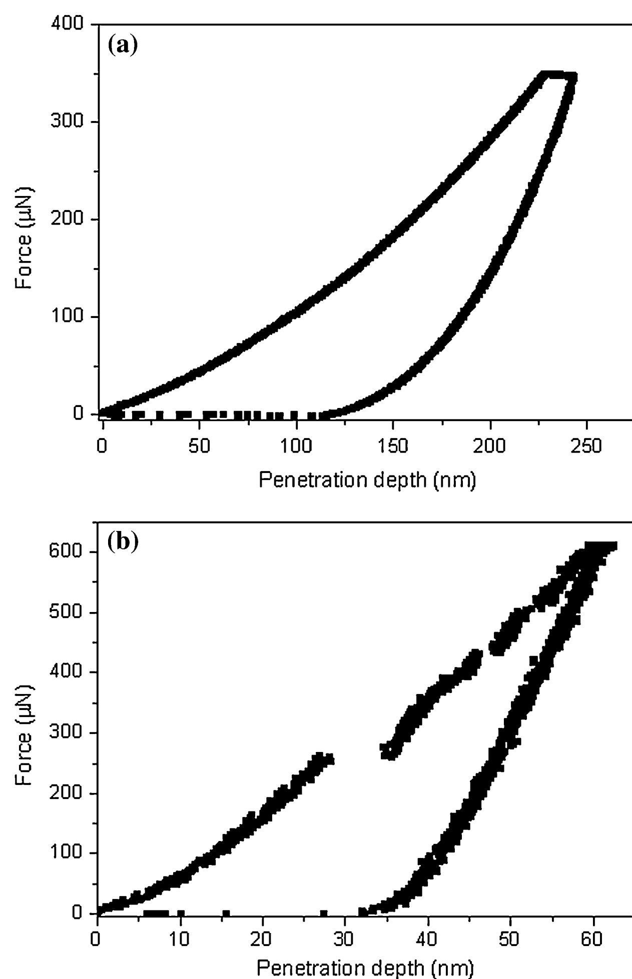

Fig. 2 Triboscope nanoindentation force versus penetration depth curves for (**a**) PMMA and (**b**) InP

nanoindentation curve for PMMA is presented in Fig. 2a. A total penetration depth of 243 nm is obtained for a maximum force of 346 µN. Creep is observed in the nanoindentation curve due to the 2 s hold time used in our nanoindenter load function. Nanoindentations were performed and the PMMA elastic modulus was achieved as 4.9 ± 0.4 GPa and its hardness was 402 ± 62 MPa.

In Fig. 2b a nanoindentation curve of InP is shown. A maximum force of 609 µN was used, reaching a total penetration depth of 62.5 nm. A discontinuity in the load part of the curve can be seen at 262 µN. Smaller discontinuities are noted for load forces above 262 µN. Its elastic modulus and hardness were measured as 89.0 ± 3.3 GPa and 8.3 ± 1.2 GPa, respectively.

In Fig. 3, AFM nanoindentation curves are shown for PMMA and InP. The nanoindentation curve for PMMA shows that the AFM tip was deeply indented on the surface. A total penetration depth of 25 nm was obtained at a maximum normal force of 13 µN. A continuous process of deformation upon load is shown and plastic deformation is

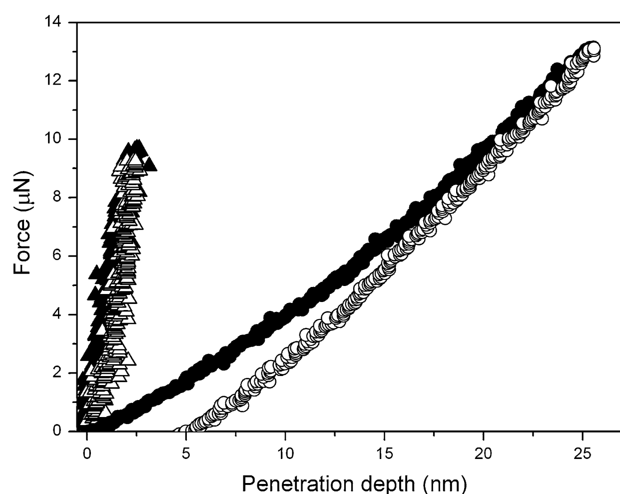

Fig. 3 AFM nanoindentation curves for PMMA (circles) and InP (triangles) measured with the stainless steel cantilever. The load curves are represented with solid symbols and the unload curves with open symbols

observed. The unload part of the nanoindentation curve was analyzed. An elastic modulus of 4.1 ± 1.2 GPa and hardness of 2.4 ± 0.7 GPa were obtained.

The nanoindentation curve for InP presented in Fig. 3, shows the load and unload curves superposed, i.e., an elastic regime is observed. A total penetration depth of 2.5 nm is obtained at a maximum indentation force of 10 µN. Its elastic modulus and maximum contact pressure were measured by the analysis of the unload part of the nanoindentation curve as 96.2 ± 12.7 GPa and 11.8 ± 2.6 GPa, respectively. Due to the InP deformation mechanism, the material's hardness is referred either as maximum contact pressure, when obtained from nanoindentation curves within an elastic deformation regime, or as hardness when obtained from curves within a plastic deformation regime. AFM nanoindentations on InP with forces above 10 µN may present discontinuities. Such discontinuities cause difficulty in the measurement of the mechanical properties by the analyses of the normal bending of the cantilever in nanoindentation curves. Therefore, to correctly analyze the AFM nanoindentations, a complete analysis of the AFM tip vertical and lateral movements is necessary.

In Fig. 4, an AFM nanoindentation curve and the respective cantilever movement during the nanoindentation on PMMA are presented. In Fig. 4a, a maximum penetration depth of 10 nm was obtained at a normal force of 3.5 µN. The load and unload curves are superposed indicating that under such a load an elastic deformation regime is observed. Figure 4b shows the movement of the laser beam, reflected on the backside of the AFM cantilever, on the AFM photodetector. The vertical and lateral movements of the laser beam on the photodetector are directly related with the cantilever normal bending and torsion

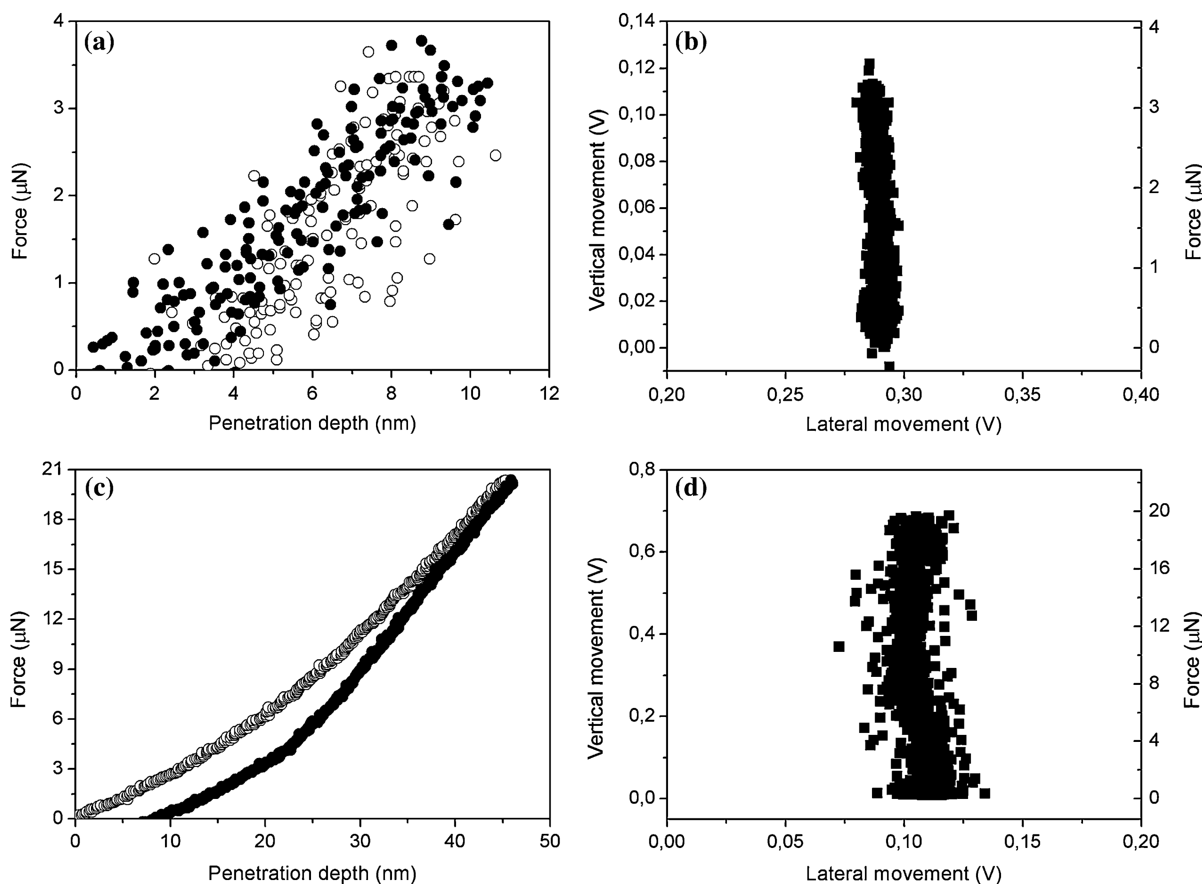

Fig. 4 AFM nanoindentation curves on PMMA. (**a**) Load versus penetration curve showing an elastic deformation regime. (**b**) The vertical and lateral movements of the laser beam on the photodetector acquired during the nanoindentation measurements shown in (**a**). (**c**) A plastic deformation regime is shown in a load versus penetration curve and the respective laser beam movement during the nanoindentation is presented in (**d**)

respectively. A 0.12 V vertical movement of the laser beam on the photodetector corresponding to a cantilever vertical movement of 10 nm is observed. No lateral movement of the laser beam is detected. In Fig. 4c, a maximum penetration depth of 45 nm was obtained at a normal force of 20 µN. A continuous process of deformation is observed during the nanoindentation. In Fig. 4d, a 0.70 V vertical movement of the laser beam on the photodetector is observed corresponding to a cantilever vertical movement of 45 nm. A vertical movement of the laser beam on the detector is seen until a nanoindentation force of 4 µN is reached. Then, as the nanoindentation force increases, both vertical and lateral movements of the laser beam on the photodetector are observed.

AFM nanoindentation curves and the movement of the microscope cantilever during nanoindentation on InP are presented in Fig. 5. In Fig. 5a, a nanoindentation curve with an elastic deformation regime is presented. A penetration depth of 3 nm is reached for a maximum applied force of 10 µN. In Fig. 5b, the vertical movement of the laser beam on the AFM photodetector is presented. A laser beam vertical movement of 0.29 V corresponds to 3 nm of cantilever vertical movement. A nanoindentation curve with maximum load of 50 µN and an indentation depth of 45 nm is shown in Fig. 5c. In Fig. 5d, the respective movement of the laser beam is presented. A 1.30 V vertical movement of the laser beam on the photodetector is observed corresponding to a cantilever vertical movement of 45 nm. The vertical movement is observed until a normal force of 25 µN is achieved. As the nanoindentation force is increased, a vertical laser movement combined with a lateral laser displacement on the photodetector is observed.

Discussion

The deformation mechanism on viscoelastic PMMA is associated with a complex motion of polymer chains. The polymer deformation under load is partially reversible. It involves the distortion of the polymer chains from their equilibrium conformations through activated segment

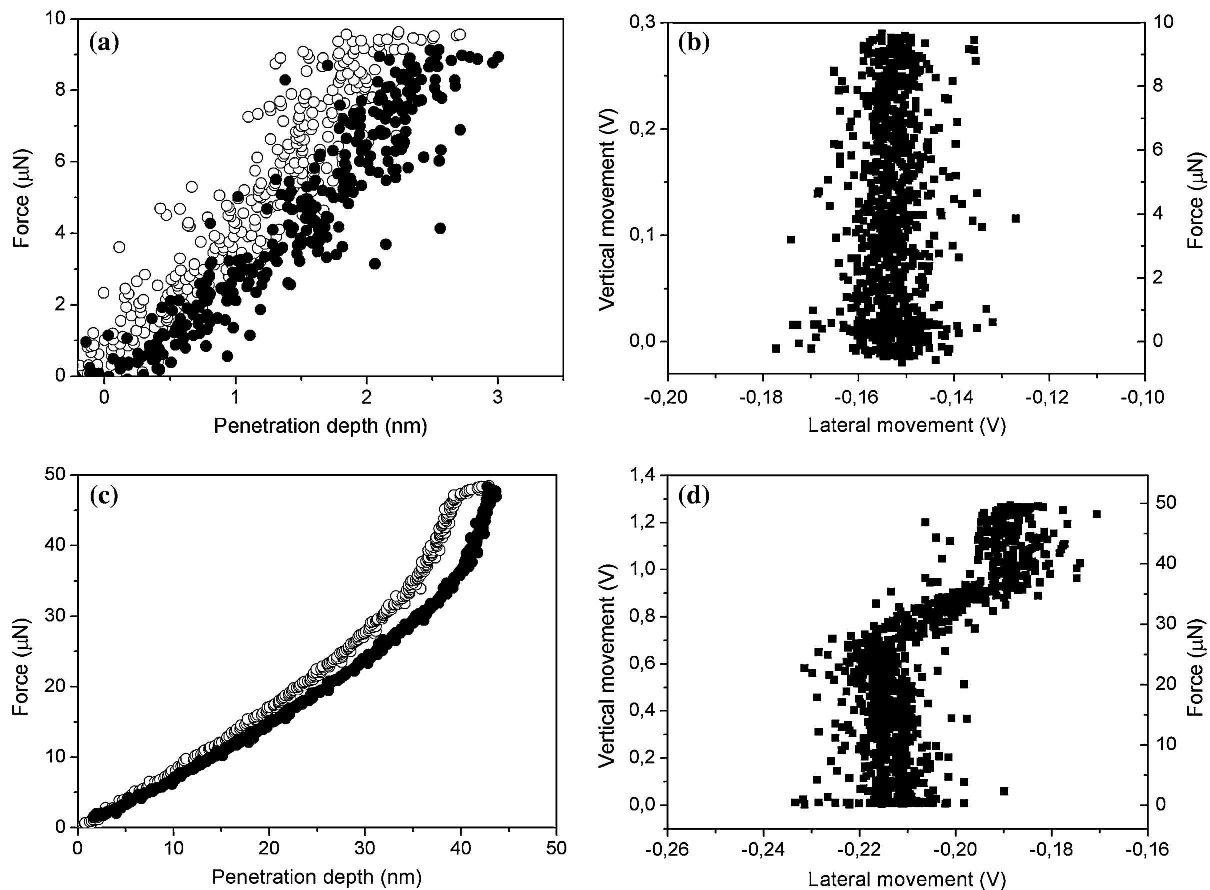

Fig. 5 AFM nanoindentation curves on InP. (**a**) Load versus penetration curve showing an elastic deformation regime. (**b**) The vertical and lateral movements of the laser beam on the photodetector acquired during the nanoindentation measurements shown in (**a**). (**c**) A plastic deformation regime is shown in a load versus penetration curve and the respective laser beam movement during the nanoindentation is presented in (**d**)

motion involving rotation about chemical bonds. Permanent deformation is associated with irreversible slippage of molecular chains past one another [10]. The PMMA deformation is a continuous process and no sudden yielding of material under load was observed in our Triboscope (Fig. 2a) or AFM nanoindentations (Fig. 3).

The PMMA elastic moduli measured by nanoindentation using either the AFM or the Triboscope system are in good agreement. On the other hand, the hardness value obtained by AFM is bigger than the value observed by nanoindentation with the Triboscope system. The nanoindentations in both cases were performed with spherical tips but with different curvature tip radius. The tip radius used with the Triboscope is $\approx$ 3 times bigger then the radius of the diamond tip used in our AFM. No influence of the tip radius in the elastic modulus measurement is observed due to the fact that the elastic deformation occurs on a large volume of the material under the indenter tip. The elastically deformed volume stores the mechanical energy of the system. As plastic deformation occurs, the energy stored in the elastically deformed volume is dissipated on the irreversible slip of the PMMA molecular chains in contact with the indenter tip. As a consequence, the materials hardness is influenced by the indenter tip radius while the materials elasticity is not. As the radius of the tip used in nanoindentation decreases, the hardness values are seen to increase. This is known as indentation size effect (ISE) [11]. In PMMA, as the radius of the spherical tip decreases, the number of molecular chains that can be pushed by the tip decreases so the material will not plastically deform so easily leading to an increase of the material hardness.

The movement of the laser beam on the microscope photodetector reveals the cantilever movement during the nanoindentation process. On PMMA, as seen in Fig. 4d, the torsion of the cantilever starts at a nanoindentation force of $\approx$ 4 μN. A simple estimative of the contact area between the tip and the PMMA surface for a contact depth 10 nm, and an applied normal force of 4 μN, shows that the pressure applied by the AFM tip is of the order of 0.8 GPa [12].

The deformation response of a material under load, to spherical indentation was described by Field and Swain

[13]. They show that the point where the plastic flow of material begins, defined as the yield stress, is equal to P/3, where P is the pressure over the contact area. The PMMA yield stress calculated, with the hardness values obtained from our AFM nanoindentations, was 0.8 ± 0.2 GPa. Thus, as shown in Fig. 4d, the lateral movement of the laser beam on the microscope photo detector, i.e., the torsion of the AFM cantilever occurs when the yield stress is achieved.

In AFM nanoindentation, the apex of the AFM tip is usually not perpendicular to the material surface. As a consequence, there is an asymmetric distribution of the applied normal force on the material beneath the tip. Therefore, as the yield stress is achieved, the plastic flow of PMMA molecular chains is more likely to occur at a tip side generating the tip torsion observed in nanoindentation experiments.

The indium phosphide elastic moduli measured by nanoindentation, using either the AFM or the Triboscope system, are in good agreement as well. The maximum contact pressure value obtained by AFM is again bigger than the hardness value obtained by nanoindentation with the Triboscope.

Indium phosphide is a semiconductor with a zinc blend crystallographic structure that mechanically deforms by the generation and propagation of dislocations. This material can deform elastically by the compression of its lattice below the indented area. Plastic deformation is presented by the slip of the preferential planes {111} causing a catastrophic event that is revealed on the nanoindentation curves as a discontinuity called pop-in [14].

In nanoindentation curves obtained with the Triboscope shown in Fig. 2b, the discontinuities are clearly seen. In AFM nanoindentation however, due to the vertical bending as well as cantilever rotation along its main axis, i.e., torsion, the pop in event introduces a distortion on the nanoindentation curve. An asymmetric distribution of the applied normal force on the material beneath the tip occurs leading to the slip of {111} planes at a tip side generating the tip torsion observed.

An analysis of the laser beam movement on the microscope photodetector, as shown in Fig. 5d, reveals that a sudden torsion of cantilever occurs in a force of ≈ 25 μN during the nanoindentation process. At this load, a penetration depth of 30 nm is observed. An estimated contact radius between the tip and the InP surface of 61 nm, shows that the pressure applied by the AFM tip is 2.1 ± 0.5 GPa.

A yield stress of 3.9 ± 0.9 GPa was calculated, following Field and Swain definition, using the contact pressure obtained from the AFM elastic curve data shown in Fig. 5a. The InP yield stress determined by the analysis of the cantilever torsion movement (≈2.1 GPa) is lower than the yield stress calculated by the AFM elastic curve (≈3.9 GPa). The yield stress calculated from the nanoindenter curves is 2.8 ± 0.4 GPa.

It is known that the plastic flow of material on semiconductors like InP occurs due to the sudden movement of dislocations on the semiconductor crystalline structure. Such semiconductor can sustain an average pressure in the contact area that is nearly twice the materials hardness before the generation of dislocations [15]. This effect cannot be explained by any error in the estimated AFM or nanoindenter contact area. Therefore, the yield stress directly determined from the elastic AFM data, as predicted by Field and Swain, is overestimate. After the generation of dislocations, the average pressure in the contact area becomes constant and is defined as the InP hardness. The abrupt cantilever torsion observed in Fig. 5d is associated with the sudden generation of dislocations in the crystal. Therefore, the yield stress obtained by the torsion of the AFM cantilever gives a better estimative of the material yield stress.

Conclusions

In this paper an analysis of the atomic force microscope tip movement during the nanoindentation process is performed. We show that the mechanical properties of materials that undergo a continuous deformation process under load like PMMA can be directly obtained from AFM nanoindentation curves. The values are comparable with values obtained with nanoindentation systems like the Triboscope used in our tests. While the hardness is affected by the tip radius used in the nanoindentation experiments, the materials elastic modulus is not influenced. The beginning of the lateral movement of the laser beam, reflected on the backside of the AFM cantilever, on the AFM photodetector is shown to occur at the material yield stress point.

AFM nanoindentations on crystalline materials that are subject to a discontinuous process of deformation under load like InP have to be carefully analyzed. AFM nanoindentation curves performed with low loads and within an elastic regime of deformation can be used on the measurement of the materials elastic modulus. The elastic moduli are comparable with the values obtained in nanoindentation systems. The effect that, before the pop-in event, such crystalline materials can sustain a pressure higher than the materials hardness is observed on the AFM nanoindentation. An analysis of the lateral movement of the laser beam associated with the cantilever torsion was used to determine the materials yield stress.

Acknowledgements This work was partially supported by the Brazilian Agencies: Conselho Nacional de Desenvolvimento Científico e Tecnológico (CNPq) and Fundação Carlos Chagas Filho de Amparo à Pesquisa do Estado do Rio de Janeiro (FAPERJ). The authors wish to thank L. Kuhn from Hysitron for fruitful discussions.

References

1. Bushan B, Koinkar VN (1994) Appl Phys Lett 64(13):1653. doi: 10.1063/1.111949
2. Garcia R, Perez R (2002) Surf Sci Rep 47:197. doi:10.1016/S0167-5729(02)00077-8
3. Cretin B, Vairac P (1998) Appl Phys A 66:S235. doi:10.1007/s003390051137
4. Tai K, Dao M, Suresh S, Palazoglu A, Ortiz C (2007) Nat Mater 6:454. doi:10.1038/nmat1911
5. Vanlandingham MR, McKnight SH, Palmese GR, Elings JR, Huang X, Bogetti TA, Eduljee RF, Gillespie JW (1997) J Adhes 64:31. doi:10.1080/00218469708010531
6. Kracke B, Damaschke B (2000) Appl Phys Lett 77(3):361. doi: 10.1063/1.126976
7. Oliver WC, Pharr GM (1992) J Mater Res 7(6):1564. doi: 10.1557/JMR.1992.1564
8. Swiss Center for Electronics and Microtechnology, AFM tip tester. http://www.csem.ch/fs/nanotech.htm, CSEM, Neuchatel, Switzerland. Last visited: 12 December 2007
9. Villarrubia JS (1997) J Res Natl Inst Stand Technol 102:425
10. Billmeyer FW (1984) Textbook of polymer science, 3rd edn. Wiley-Interscience, New York
11. Swadener JG, George EP, Pharr GM (2002) J Mech Phys Solids 50:681. doi:10.1016/S0022-5096(01)00103-X
12. Hyon CK, Choi SC, Hwang SW, Ahn D, Young K, Kim EK (1999) Appl Phys Lett 75:292. doi:10.1063/1.124351
13. Field JS, Swain MV (1993) J Mater Res 8(2):297. doi:10.1557/JMR.1993.0297
14. Bourhis Le E, Patriarche G (2003) Prog Cryst Growth Charact Mater 47:1. doi:10.1016/j.pcrysgrow.2004.09.001
15. Bradby JE, Williams JS, Wong-Leung J, Swain MV, Munroe P (2001) Appl Phys Lett 78:3235. doi:10.1063/1.1372207